Applied Geochemistry 66 (2016) 198–209

Contents lists available at ScienceDirect

Applied Geochemistry

journal homepage: www.elsevier.com/locate/apgeochem

Processes controlling ^{234}U and ^{238}U isotope fractionation and helium in the groundwater of the St. Lawrence Lowlands, Quebec: The potential role of natural rock fracturing

Pauline Méjean*, Daniele L. Pinti, Marie Larocque, Bassam Ghaleb, Guillaume Meyzonnat, Sylvain Gagné

GEOTOP and Département des sciences de la Terre et de l'atmosphère, Université du Québec à Montréal, CP888, Succ. Centre-Ville, Montréal, QC H3C 3P8, Canada

ARTICLE INFO

Article history:
Received 25 July 2015
Received in revised form
14 December 2015
Accepted 23 December 2015
Available online 29 December 2015

Keywords:
$(^{234}U/^{238}U)$ activity ratio
Helium isotopes
Fractured aquifers
α-recoil
^{4}He excess
St. Lawrence Lowlands

ABSTRACT

The goal of this study is to explain the origin of ^{234}U–^{238}U fractionation in groundwater from sedimentary aquifers of the St. Lawrence Lowlands (Quebec, Canada), and its relationship with $^{3}He/^{4}He$ ratios, to gain insight regarding the evolution of groundwater in the region. $(^{234}U/^{238}U)$ activity ratios, or $(^{234}U/^{238}U)_{act}$, were measured in 23 groundwater samples from shallow Quaternary unconsolidated sediments and from the deeper fractured regional aquifer of the Becancour River watershed. The lowest $(^{234}U/^{238}U)_{act}$, 1.14 ± 0.01, was measured in Ca–HCO_3-type freshwater from the Quaternary Shallower Aquifer, where bulk dissolution of the carbonate allows U to migrate into water with little ^{234}U–^{238}U isotopic fractionation. The $(^{234}U/^{238}U)_{act}$ increases to 6.07 ± 0.14 in Na–HCO_3–Cl-type groundwater. Preferential migration of ^{234}U into water by α-recoil is the underlying process responsible for this isotopic fractionation. An inverse relationship between $(^{234}U/^{238}U)_{act}$ and $^{3}He/^{4}He$ ratios has been observed. This relationship reflects the mixing of newly recharged water, with $(^{234}U/^{238}U)_{act}$ close to the secular equilibrium and containing atmospheric/tritiogenic helium, and mildly-mineralized older water (^{14}C ages of 6.6 kyrs), with $(^{234}U/^{238}U)_{act}$ of ≥6.07 and large amounts of radiogenic ^{4}He, in excess of the steady-state amount produced *in situ*. The simultaneous fractionation of $(^{234}U/^{238}U)_{act}$ and the addition of excess ^{4}He could be locally controlled by stress-induced rock fracturing. This process increases the surface area of the aquifer matrix exposed to pore water, from which produced ^{4}He and ^{234}U can be released by α-recoil and diffusion. This process would also facilitate the release of radiogenic helium at rates greater than those supported by steady-state U–Th production in the rock. Consequently, sources internal to the aquifers could cause the radiogenic ^{4}He excesses measured in groundwater.

1. Introduction

Knowledge of groundwater flow velocities and residence times is critical to the quantification of pollutant migration (Gascoyne, 2004) and aquifer vulnerability (Meyzonnat et al., 2015). Flow velocities can be determined using *in situ* tracer tests (Geyh, 2005) or aquifer materials in the laboratory (Andersen et al., 2009; Bonotto and Andrews, 2000). Such methods provide local estimates of groundwater velocity and do not take the natural heterogeneity of an aquifer system at the regional scale into account. Studies performed at the watershed scale can partially account for this heterogeneity by integrating information from a large set of isotopic groundwater ages (Phillips and Castro, 2003). However, chronometers such as ^{14}C (Plummer and Glynn, 2013) can be affected by water–rock interactions and their chronological information can be altered or partially lost as a result.

In this regard, the ratio of ^{234}U and ^{238}U activities, $(^{234}U/^{238}U)_{act}$, has the potential to quantify such water–rock interactions (e.g., Riotte and Chabaux, 1999; Riotte et al., 2003; Fröhlich, 2013; Paces and Wurster, 2014). Since the pioneering work of Cherdyntsev et al. (1955), it has been shown that groundwater almost always has a $(^{234}U/^{238}U)_{act}$ greater than one, the value corresponding to secular equilibrium, at which the activity of the daughter nuclide is equal to the activity of the parent nuclide. The physical process responsible

* Corresponding author.
E-mail address: mejean.pauline@courrier.uqam.ca (P. Méjean).

http://dx.doi.org/10.1016/j.apgeochem.2015.12.015
0883-2927/

for the ^{234}U–^{238}U fractionation is the α–decay of ^{238}U. During decay, α-particles are emitted, transmitting kinetic energy to the ^{238}U-daughter nuclide, ^{234}Th. ^{234}Th is displaced 30–100 μm from its original site, and a fraction of the ^{234}Th is ejected from the mineral grain into the pore water. The insoluble ^{234}Th is rapidly adsorbed on the grain surface and decays to ^{234}U, with a half-life of 24.1 days. The resulting ^{234}U, now residing in damaged crystal lattice sites or on grain surfaces, will be transferred in its soluble form into the water phase (Kigoshi, 1971).

The extent of this ^{234}U–^{238}U fractionation depends on numerous aquifer parameters, such as path lengths, grain surface of the porous media (Tricca et al., 2001; Maher et al., 2006), fracture surface and the duration of the recoil process (Andrews et al., 1982; Andrews, 1983), chemical aggression capacity, mineralogical composition of the rock in contact with water, the water/rock ratio (Riotte and Chabaux, 1999; Paces et al., 2002; Riotte et al., 2003; Durand et al., 2005), and/or the contact time between flowing water and the aquifer matrix (Elliot et al., 2014). The behavior of ^{234}U compared with that of its parent, ^{238}U, is therefore useful for tracing groundwater flow patterns (Kronfeld et al., 1979; Osmond and Cowart, 1976, 1982, 2000), determining mixing volumes and rates between waters of different ages (e.g., Andrews and Kay, 1983; Tricca et al., 2000), and identifying groundwater inflow into surface waters (Plater et al., 1992; Durand et al., 2005).

Because of the long half-life of ^{234}U (2.46×10^5 yrs), many attempts have been made to apply the $(^{234}U/^{238}U)_{act}$ to the dating of old groundwater up to hundreds of thousands of years in age (Osmond et al., 1974; Andrews et al., 1982; Andrews and Kay, 1983; Fröhlich and Gellermann, 1987; Ivanovitch et al., 1991). However, the majority of these studies have shown that the excess decay of ^{234}U may not reflect groundwater residence times, but rather uranium redistribution between the aquifer matrix and the water phase. Consequently, to obtain reliable residence times, the method requires a detailed knowledge of the aquifer characteristics, such as matrix grain size and fracture openings (Andrews, 1983; Andrews et al., 1982; Tricca et al., 2001), as well as the adsorption of these isotopes onto the aquifer matrix (Fröhlich and Gellermann, 1987; Porcelli and Swarzenski, 2003).

Radiogenic helium isotopes in groundwater are produced by neutron reactions with Li (^3He) and α-decay of U and Th (^4He) contained in the aquifer rocks (e.g., Kulongoski and Hilton, 2011). Compared with U-isotopes, He-isotopes are insensitive to redox conditions, chemical reactions, and adsorption processes, given that helium is a noble gas. The mixing of water masses with different ages and provenance primarily controls the helium isotopic variability in a groundwater system (e.g., Vautour et al., 2015; Saby et al., 2016). Groundwater ages, calculated from the radiogenic ^4He accumulation rate in water, are often higher than the hydrological ages, indicating an excess of ^4He (e.g., Pinti and Marty, 1998; Kulongoski and Hilton, 2011; Torgersen and Stute, 2013). Additional sources of radiogenic ^4He could be related to He basal fluxes entering the aquifers (e.g., Torgersen and Clarke, 1985) or the release of ^4He from the aquifer rock at rates greater than those supported by steady-state U–Th production in rocks (Solomon et al., 1996).

The objective of this study is to explain the cause of ^{234}U–^{238}U fractionation in the St. Lawrence Lowlands (Fig. 1) aquifers, to better understand the evolution of groundwater in the region. It is one of the first attempts to examine the relationships between U and He isotopes, and how these may be linked in groundwater environments.

2. Study area

2.1. Geology and hydrogeology

The study area (2859 km^2) is located in southern Quebec (Fig. 1a), encompassing the lower portion of the Becancour River watershed, as well as eight smaller watersheds feeding the St. Lawrence River. The northwestern part of the watershed corresponds geographically to the St. Lawrence Lowlands, a flat area less than 150 m asl. The southeastern part of the watershed is located in the Appalachian Mountains, characterized by irregular topography reaching maximal elevations of approximately 500 m (Fig. 1b). These two regions correspond geologically to the Cambro-Ordovician sedimentary St. Lawrence Platform and the Cambro-Devonian metasedimentary Appalachian Mountains respectively.

The St. Lawrence Platform is a 1200 m-thick sequence of Cambrian-Early Ordovician siliciclastic and carbonate sediments, overlain by 1800 m of Middle-Late Ordovician foreland carbonate-clastic-shale deposits (Lavoie, 2008). Ordovician geological units outcropping in the lower part of the Becancour watershed are: 1) red shale interbedded with green sandstone and lenticular gypsum of the Queenston Group, and 2) mudstone, sandstone, and silty shale turbiditic units of the Lorraine and Sainte Rosalie Groups (Fig. 1b). Dominant terrains in the Appalachian Mountains correspond to imbricated thrust sheets produced during the Taconian Orogeny: 1) Cambrian green and red shales (Sillery Group), 2) Ordovician bedded black and yellowish-weathered shaly matrix containing chaotic blocks of shales, cherts, and sandstone forming the "wildflysch" of the Etchemin River Olistostrome, and 3) Middle Ordovician dolomitic or calcitic schists of the Sweetsburg and the West Sutton Formation of the Oak Hill Group (Globensky, 1993) (Fig. 1b).

Unconsolidated Quaternary sediments derived from the last two glaciation–deglaciation cycles unconformably cover the Cambrian-Ordovician sedimentary sequence of the St. Lawrence Platform (Lamothe, 1989). A nearly continuous till sheet (Gentilly till) covers most of the area, separating the lacustrine and deltaic patches of sand deposited during marine regressions (Vieilles Forges and Lotbinière sands; Lamothe, 1989) from the uppermost clay units of the Champlain Sea (11.1–9.8 ka; Occhietti et al., 2001; Occhietti and Richard, 2003).

During the last deglaciation, the retreat of the Laurentide Ice Sheet caused a marine invasion from the Gulf of St. Lawrence, called the Champlain Sea episode. This water is a mixture of meltwater from the Laurentide Ice Sheet and seawater (Hillaire-Marcel and Causse, 1989). Glacio-marine sediments of the Champlain Sea are found between the elevations of 175 and 65 m (Godbout, 2013; Parent and Occhietti, 1988). Generally encountered below 100 m elevation in ancient channels, the Champlain Sea clay can be more than 40 m thick in the Chambly–Fortierville syncline, close to the St. Lawrence River (Fig. 1b). Glacio-marine deltaic sandy sediments are mainly found along the Becancour River, at elevations between 65 and 100 m asl.

In the study area, two distinct aquifer systems are apparent: 1) a regional fractured bedrock aquifer in the Middle-Late Ordovician sedimentary units of the St. Lawrence Platform, and 2) discontinuous and localized perched aquifers in the fluvio-glacial sands of the Quaternary Vieilles Forges Formation (hereafter referred to as "granular aquifers") (Larocque et al., 2013). The main recharge zones of the regional fractured aquifer are located in the Appalachian Mountains. Local recharge has been observed in the lower part of the basin, downhill, where Champlain Sea clays are absent (Larocque et al., 2013). Groundwater flows from the Appalachian Mountains northwesterly to the St. Lawrence River (Fig. 1a). The Becancour River acts as the main discharge for the regional fractured bedrock aquifer. The hydraulic conductivities of the fractured bedrock aquifer are low to moderate (~10^{-9}–10^{-6} m s^{-1}). Effective porosity varies between 1 and 5% for the Ordovician fractured regional aquifer (Tran Ngoc, 2014) and between 10 and 20% for the Quaternary granular aquifer (Benoit et al., 2011).

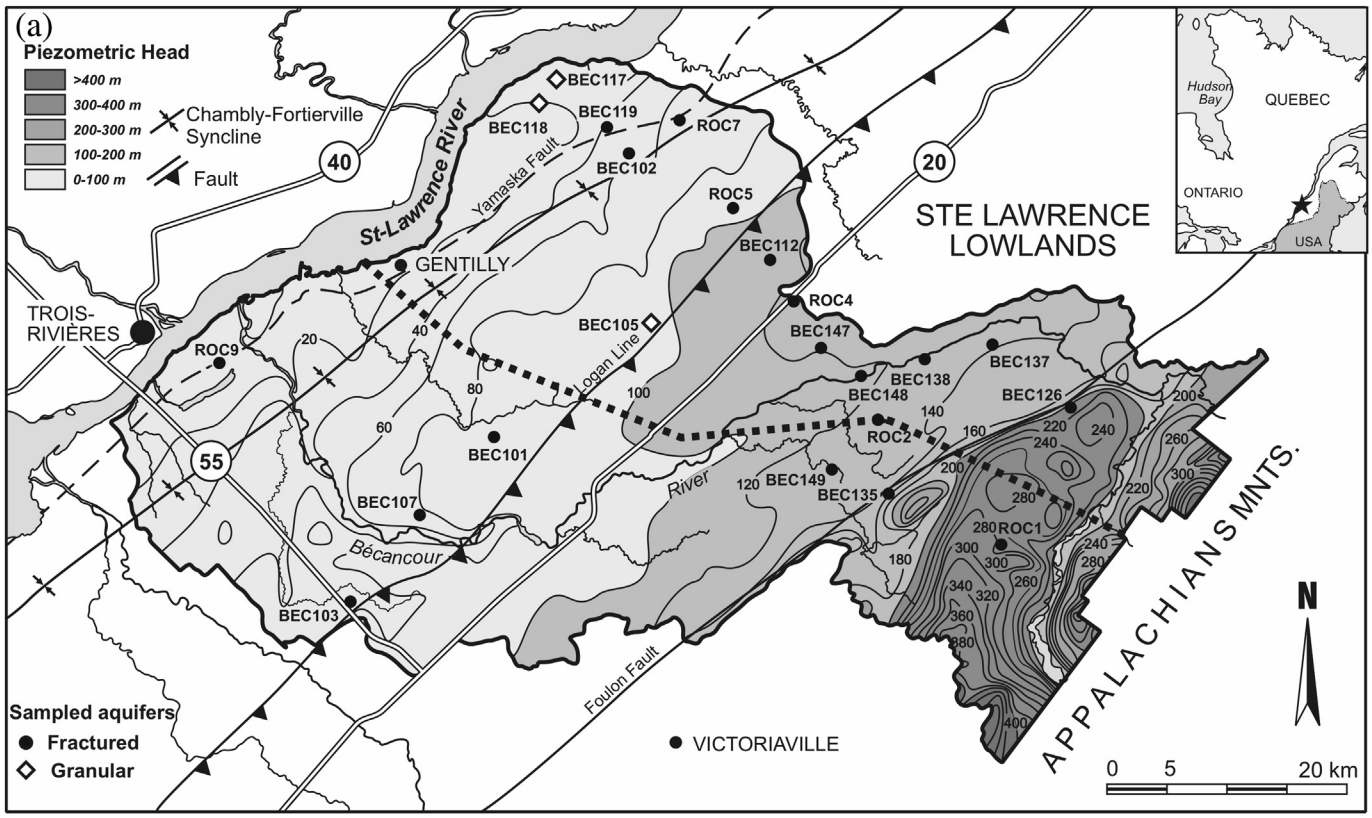

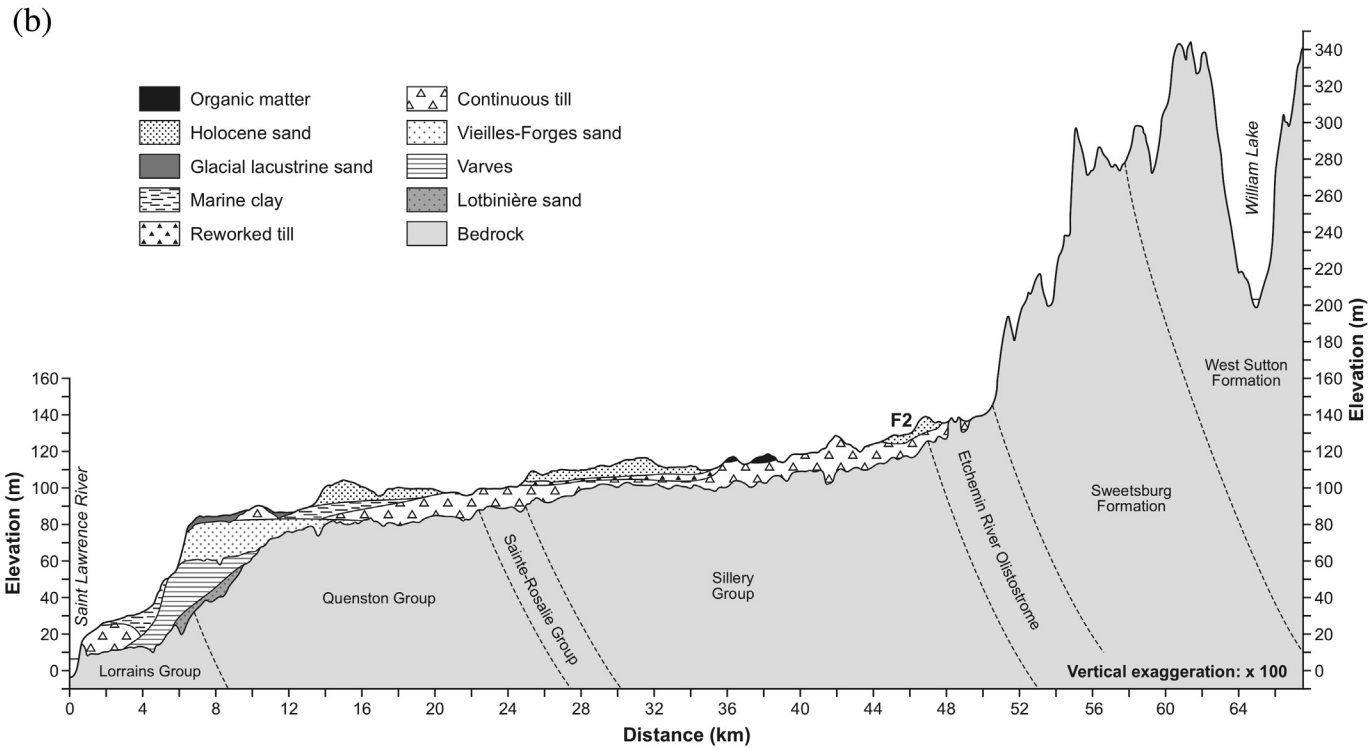

Fig. 1. (a) Simplified map of the Becancour watershed, southern Quebec, with potentiometric head isolines of the regional fractured bedrock aquifer and the groundwater sampled wells of this study (diamonds: Quaternary granular aquifer; circles: Ordovician regional fractured bedrock aquifer). (b) Cross section illustrating shallow granular aquifers and deeper fractured aquifers with geological groups belonging to the St. Lawrence Platform and the Appalachian Mountains.

Table 1
Hydrogeological characteristics of the groundwaters sampled in the Becancour River watershed together with U-series isotopic data.

Sample	Water chemistry	Hydrological conditions	Depth m	Geological province	Geology group/Fm.	Temp °C	pH	[U] ppb	±	$(^{234}U/^{238}U)_{act}$	±	$[^4He]$ cm^3 STP g^{-1} $\times 10^{-8}$	±	$\frac{(^3He/^4He)_{sample}}{(^3He/^4He)_{air}}$	±	Alkalinity mg L^{-1} HCO_3	TDS mg L^{-1}	Ca	Mg	K	Na	Cl	SO_4	HCO_3^-	SI calcite
BEC101 (F)	Na−HCO_3,Cl	Confined	47.2	SL Platform	Lorraine	12	9.17	0.044	0.0004	6.07	0.14	1169.41	17.54	0.074	0.003	414.8	780	1.2	0.29	1.1	210	150.0	2.2	414.8	0.21
BEC102 (F)	Ca−HCO_3	Semi-confined	21.6	SL Platform	Queenston	8.9	7.44	0.029	0.0003	2.50	0.01	7.95	0.12	2.316	0.048	268.4	427	55.0	8.3	2.4	44	37.0	12.0	268.4	−0.07
BEC103 (F)	Ca−HCO_3	Unconfined	43.6	SL Platform	Sainte-Rosalie	9.6	7.21	0.244	0.004	3.47	0.02	63.35	0.95	0.381	0.011	268.4	501	73.0	13	3.1	40	62.0	41.0	268.4	−0.19
BEC105 (G)	Ca−HCO_3	unconfined	7.0	SL Platform	Sainte-Rosalie	9.4	6.00	0.247	0.002	1.26	0.01	9.23	1.40	0.788	0.021	104.9	213	30.0	3.2	1.2	24	35.0	15.0	104.9	−2.13
BEC107 (F)	Ca−HCO_3	Unconfined	36.6	SL Platform	Lorraine	13.3	8.13	2.939	0.012	1.55	0.005	39.65	0.59	0.412	0.009	101.3	188	33.0	5.4	0.82	5.8	9.6	32.0	101.3	0.09
BEC110 (F)	Ca−Na,SO_4	Confined	37.8	SL Platform	Queenston	8.9	8.03	0.122	0.001	n.d.	n.d.	60.65	0.91	0.172	0.008	160.0	346	43.0	11	1.8	29	5.8	60.0	195.2	0.28
BEC112 (F)	Ca−HCO_3	unconfined	38.1	Appalachian Mts	Stanbridge	8.6	7.76	0.046	0.0002	2.11	0.02	6.70	0.10	1.238	0.041	207.4	286	32.0	11	2	24	1.7	8.1	207.4	−0.07
BEC117 (G)	Ca−HCO_3	unconfined	15.2	SL Platform	Lorraine	7.4	6.83	0.090	0.0003	1.69	0.02	5.36	0.08	1.604	0.010	70.8	84	22.0	2	0.53	2.3	0.8	8.8	57.3	−1.69
BEC118 (G)	Ca−HCO_3	Unconfined	6.1	SL Platform	Lorraine	9.9	6.17	0.027	0.0002	1.14	0.01	6.04	0.09	1.077	0.037	57.3	298	15.0	1.5	0.29	3.2	2.2	4.8	170.8	−2.01
BEC119 (F)	Na−HCO_3,Cl	Semi-confined	45.7	SL Platform	Lorraine	12.0	7.38	0.003	0.00002	5.15	0.15	62.92	0.94	0.283	0.014	170.8	471	21.0	6.9	2.6	53	43.0	1.0	292.8	−0.44
BEC126* (F)	Ca−HCO_3	Unconfined	49.1	Appalachian Mts	Olistostrome*	8.8	7.71	0.111	0.001	2.69	0.14	2662 −4482	67.23	0.039	0.003	134.2	227	25.0	6.2	0.9	27	26.0	7.6	134.2	−0.4
BEC135 (F)	Ca−HCO_3	Unconfined	44.2	Appalachian Mts	Sillery	8.9	5.06	0.159	0.001	3.85	0.03	n.d.	n.d.	n.d.	n.d.	170.8	85	54.0	6.1	0.97	3.8	1.9	18.0	170.2	nd
BEC137 (F)	Na−HCO_3	Semi-confined	23.7	Appalachian Mts	Sillery	8.6	8.13	0.044	0.0003	2.47	0.04	11.32	0.17	0.720	0.019	219.6	350	5.1	0.41	1.6	85	9.4	29.0	219.6	−0.47
BEC138 (F)	Ca−HCO_3	Unconfined	32.0	Appalachian Mts	Sillery	8.9	7.10	0.028	0.003	1.77	0.02	7.72	0.12	2.005	0.039	158.6	216	42.0	3.3	1.4	6	2.7	2.4	158.6	−0.71
BEC147 (F)	Ca−HCO_3	Unconfined	32.0	Appalachian Mts	Olistostrome*	9.9	7.63	1.502	0.009	2.93	0.08	7.51	0.11	1.341	0.033	268.4	157	56.0	6.9	5.6	47	13.0	28.0	268.4	nd
BEC148 (F)	Ca, Na−SO_4	Unconfined	64.6	Appalachian Mts	Sillery	10.4	8.81	0.237	0.001	2.59	0.03	12.38	0.19	0.711	0.014	n.d.	109	7.4	1.3	1.4	72	1.5	25.0	nd	nd
BEC149 (F)	Ca−HCO_3	Unconfined	54.9	Appalachian Mts	Sillery	9.5	5.16	0.198	0.001	3.03	0.02	97.84	1.47	0.344	0.010	195.2	286	50.0	4	2	15	5.7	14.0	195.2	−2.49
F1 (F)	Ca−Na,SO_4	Unconfined	30.0	Appalachian Mts	Oak hill	8.5	5.99	0.071	0.001	2.55	0.69	77.28	1.16	0.996	0.019	31.7	62	13.0	2	0.64	3.4	2.2	9.5	31.7	−2.98
F2 (F)	Ca−Na,SO_4	Unconfined	42.0	Appalachian Mts	Sillery	7.2	9.38	0.278	0.001	3.87	0.02	21.22	0.32	0.386	0.010	n.d.	131	3.3	0.7	0.99	88	1.4	37.0	n.d.	nd
F4 (F)	Na−HCO_3	Unconfined	36.6	SL Platform	Stanbridge	8.5	9.12	0.016	0.001	3.40	0.08	62.30	0.93	1.043	0.038	207.4	339	6.8	3.3	0.83	85	2.4	33.0	207.4	0.61
F5 (F)	Na−HCO_3	Confined	47.2	SL Platform	Lorraine	8.0	9.10	0.039	0.0002	4.08	0.05	12.77	0.19	0.564	0.020	366.0	529	1.9	0.53	1.6	140	3.0	16.0	366.0	0.25
F7 (F)	Na−HCO_3,Cl	Confined	48.8	SL Platform	Lorraine	n.d.	9.29	0.148	0.001	3.79	0.01	14.40	0.24	n.d.	n.d.	305.0	150	2.5	0.67	1.1	97	1.0	7.5	303.8	nd
F9 (F)	Na−HCO_3,Cl	Unconfined	35.7	SL Platform	Lorraine	8.5	9.10	0.020	0.0001	5.88	0.02	272.50	4.09	0.058	0.002	829.6	222	3.1	2.6	3.4	590	420.0	7.5	134.2	−0.08

Notes:
(F) = Ordovician fractured bedrock aquifer; (G) Quaternary granular aquifer.
SL Platform = St. Lawrence Platform.
* Olistostrome de la Rivière Etchemin Group.
n.d.: not determined.
Helium amounts and isotopic ratios are reported from Vautour et al. (2015).
$(^3He/^4He)_{air} = 1.386 \times 10^{-6}$ (Ozima and Podosek, 1983).

2.2. Groundwater chemistry and ages

Groundwater chemistry shows the occurrence of low-salinity water with total dissolved solids (TDS) ranging from 0.06 to 0.78 g L^{-1} (Table 1). Based on major ion concentrations, Meyzonnat et al. (2015) identified three water types in the Becancour groundwater: 1) Ca–HCO_3, and Ca–HCO_3–SO_4 freshwater close to the recharge zone of the Appalachian mountains, 2) mixed water types (Na–HCO_3 and Na–HCO_3–SO_4) in the piedmont of the Appalachian Mountains and the St. Lawrence Plain, and 3) more highly mineralized waters (Ca–HCO_3–Cl–Na and Na–HCO_3–Cl types) closer to the St. Lawrence River (Meyzonnat et al., 2015). The majority of water recharged in the Appalachian Mountains has a calcite saturation index (SI, with an uncertainty of ±0.1 units; Table 1) of 2.98 and −0.07, indicating that it ranges from under-saturated in calcite to close to saturation. From this, it can be concluded that the dissolution of calcite within the aquifers is the dominant process controlling the chemistry of these waters. Groundwater reaches calcite saturation and evolves towards Na–HCO_3 type through ion exchange, where $Ca^{2+}{}_{water}$ exchanges with $Na^{+}{}_{mineral}$ in semi-confined aquifers (Fig. 2a) (Cloutier et al., 2006; Meyzonnat et al., 2015). Groundwater finally evolves to a Na–Cl type (Fig. 2a) through exchange with pore water of marine origin trapped in the Champlain Sea clays or in the fractured rock aquifers, especially in areas confined by thick marine clay and with limited water recharge (Meyzonnat et al., 2015). These saline waters are found mainly in the Lorraine Group units, and waters are located in the lowermost part of the watershed, along the Chambly–Fortierville syncline, a narrow band of 10 km parallel to the St. Lawrence River. None of these Na–Cl waters were sampled for this study.

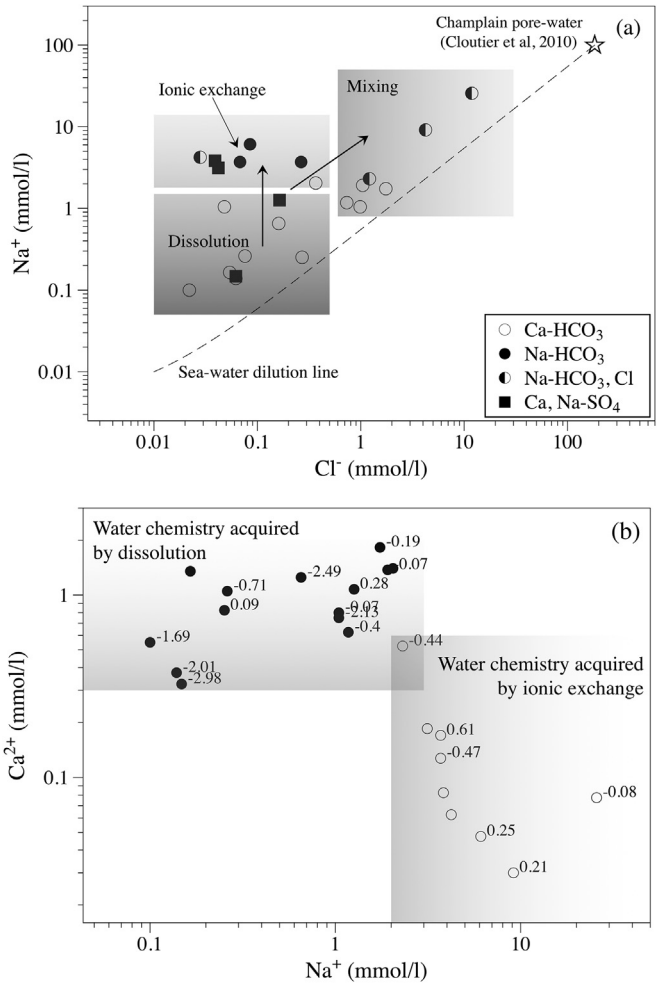

Fig. 2. (a) Plot of sodium (Na^+) versus Chloride (Cl^-) concentrations, showing the evolution of groundwater composition: Ca–HCO_3 (white dots) and Ca,Na–SO_4 (black squares) type achieved through rock dissolution, Na–HCO_3 (black dots) through ionic exchange, and Na–HCO_3–Cl (black and white dots) through mixing with older mineralized waters; (b) Logarithmic plot of Sodium (Na^+) versus Calcium (Ca^{2+}) for groundwater that is under-saturated to saturated in calcite (black dots) and groundwater saturated to oversaturated with respect to calcite (white dots). Plotted values are the calcite saturation index (SI; Table 1).

Mixing between a freshwater Ca–HCO_3 end-member and locally evolved Na–HCO_3–Cl water end-member is responsible for the geochemical character of the groundwater and its spatial distribution in the Becancour watershed (Vautour et al., 2015). This mixing is reflected in the apparently contradictory $^3H/^3He$ and ^{14}C ages measured in the same water samples from Becancour (Vautour et al., 2015) and neighboring watersheds (Saby et al., 2016). $^3H/^3He$ ages span from 2 to 60 yrs, while the NETHPATH ^{14}C-adjusted ages for the same water ranges from 6.6 thousand years to present. This apparent contradiction in age results from the mixing of old groundwater with modern water, as clearly demonstrated by Saby et al. (2016) through a linear mixing trend between the ^3H and A^{14}C activities in the St. Lawrence Lowlands groundwater, including those from the Becancour watershed.

3. Sampling and analytical procedures

Twenty-three groundwater samples were collected from municipal and domestic wells (named BEC in Fig. 1a and Table 1; n = 17) and from instrumented wells drilled for monitoring purposes (named F1, F2, F4, F5, F7 and F9 in Fig. 1a; n = 5). Sampling was done during the summers of 2012 and 2013. Twenty of the wells tap groundwater from the regional Ordovician fractured aquifer (with depths ranging from 15.0 to 64.6 m; Table 1). These are cased in the section crossing the unconsolidated Quaternary deposits and have open boreholes in the fractured bedrock. Three wells (BEC105, BEC117, and BEC118) have casings and a screen at their base, and tap groundwater from the shallower Quaternary sandy aquifer (with depths ranging from 6.1 to 15 m; Table 1).

Groundwater was collected from domestic wells using a Waterra® Inertial Pump System, which consists of a foot valve fixed to the bottom of a high-density polyethylene tube with a variable diameter of between 5/8″ to 2″ and an electric actuator Hydrolift-2® pump. Water was collected at the closest water faucet, prior to any intermediate reservoirs for the chemical treatment of the water. In municipal wells, water was collected directly at the wellhead. Water was purged from the wells until chemo–physical parameters (conductivity, pH, and temperature) stabilized. Samples were collected for uranium analyses in 1 L Nalgene© bottles filtered through 0.7 μm Millipore filters and acidified with nitric acid to a pH of around 2.

U extraction was performed at the Radioisotope laboratory of GEOTOP, following a method modified from that of Edwards et al. (1987). A known amount of spike (^{233}U–^{236}U) was added to 75 ml of water sample to determine the U concentration by isotope dilution (Chen et al., 1986). An aliquot was prepared with 150 ml of water sample following the same technique to measure $(^{234}U/^{238}U)_{act}$. Approximately 3 mg of Fe carrier ($FeCl_3$ already purified of any trace of uranium) was added to this solution, and a $Fe(OH)_3$ precipitate was created by adding a solution of ammonium hydroxide until a pH of between 7 and 9 was obtained. The precipitate was recovered by centrifugation and then dissolved in 2 ml of 6 M HCl solution and loaded in 2 ml of AG-1X8 anionic resin bed.

After washing the resin with 8 ml of 6 M HCl, the U–Fe fractions were retrieved by elution with 8 ml of H_2O and evaporated to dryness. The resulting U separate was purified using 0.2 ml U-Teva (Eichrom Industries) resin. The Fe was eluted with 3 N HNO_3 and the U fraction with 0.02 N HNO_3.

The recovered U fraction was deposited on a Rhenium filament between two layers of graphite, and U isotopes were measured with a VG-SECTOR Thermo-Ionization Mass Spectrometer (TIMS) equipped with an ion counter. Uranium concentration was determined by peak jumping between ^{236}U, ^{235}U and ^{233}U on the ion counter and corrected for mass fractionation using a double spike with a ($^{236}U/^{233}U$) of 1.132 and assuming a constant $^{238}U/^{235}U$ ratio of 137.88. To obtain $^{234}U/^{238}U$ activity ratios, we measured ^{234}U, ^{235}U, and ^{238}U and their atomic ratios on un-spiked samples. The $^{234}U/^{238}U$ atomic ratio was converted to $(^{234}U/^{238}U)_{act}$ using $\lambda^{238}/\lambda^{234} = 5.4887 \times 10^{-5}$. The analytical errors on the U concentrations were usually less than 1% (except for samples BEC138 and F4; Table 1), at the 2σ level. The errors on the $(^{234}U/^{238}U)_{act}$ vary from 0.4 to 5% with an average error of ~1.3% at 2σ level (except sample F1; Table 1).

Water samples for helium isotopic analyses were collected from the wells with 3/8-inch diameter, refrigeration-type copper tubes, cold-sealed with clamps, following standard procedures described in Vautour et al. (2015). Helium isotopes were measured at the Noble Gas Laboratory at the University of Michigan using a MAP-215 noble gas mass spectrometer. Details of the analytical procedures, uncertainties, and reproducibility are reported elsewhere (Castro et al., 2009; Vautour et al., 2015).

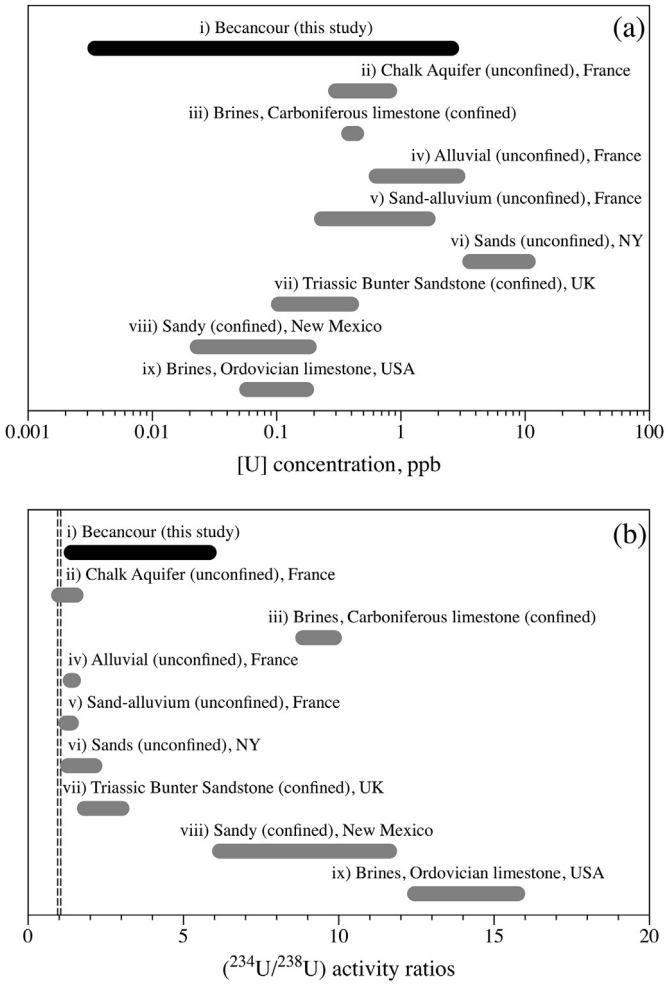

Fig. 3. Measured uranium concentrations (in ppb) and $(^{234}U/^{238}U)_{act}$ in Becancour watershed groundwater, compared to data from other sedimentary aquifers with similar lithological and hydrological conditions. Dotted vertical lines represent the $(^{234}U/^{238}U)_{act}$ secular equilibrium value.

4. Results

The uranium concentrations in ppb [U] and the activity ratios, $(^{234}U/^{238}U)_{act}$, measured in this study are reported in Table 1, together with geological and water chemistry data for the same samples, previously reported by Meyzonnat et al. (2015) and Larocque et al. (2013). ^4He amount and helium isotopic ratios ($^3He/^4He$) are reported from Vautour et al. (2015).

The measured [U] are very low and display a high degree of variability, with values ranging from 0.003 ± 0.00002 to 2.939 ± 0.012 ppb (Fig. 3a). The $(^{234}U/^{238}U)_{act}$ ratios are greater than one (i.e., exceed secular equilibrium), ranging from 1.14 ± 0.01 to 6.07 ± 0.14 (Table 1). Table 1 also reports the $^3He/^4He$ ratios measured for the samples and reported previously in Vautour et al. (2015). ^4He amounts range from 5.36×10^{-8} $cm^3STP\ g^{-1}_{H2O}$ to 4.48×10^{-5} $cm^3STP\ g^{-1}_{H2O}$ (Table 1). The lowest amount is very close to that of atmospheric helium dissolved in freshwater at the recharge (ASW or Air Saturated Water at 10 °C; 4.59×10^{-8} $cm^3STP\ g^{-1}_{H2O}$) and increases to 3 orders of magnitude higher, indicating significant accumulations of radiogenic ^4He (Vautour et al., 2015). The helium isotopic ratios ($^3He/^4He$) in groundwater, normalized to the ($^3He/^4He$) in the atmosphere (1.386×10^{-6}; Ozima and Podosek, 1983), range from 2.005 ± 0.039 to 0.039 ± 0.003. The ratios higher than the atmospheric value are explained by the addition of ^3H-produced ^3He, while the very low ratios reflect the large addition of radiogenic ^4He (Vautour et al., 2015). A detailed discussion on the helium isotopic systematics is beyond the scope of this paper and is reported in Vautour et al. (2015).

Fig. 3 compares the measured [U] and $(^{234}U/^{238}U)_{act}$ in the current study area with those from other sedimentary aquifers characterized by similar lithologies and confinement conditions (except for confined oil brines; Kronfeld et al., 1975; Banner et al., 1990). Both measured [U] (Fig. 3a) and $(^{234}U/^{238}U)_{act}$ (Fig. 3b) from the study area are within the range of values observed in other unconfined and confined sedimentary aquifers (Banner et al., 1990; Bonotto and Andrews, 2000; Durand et al., 2005; Hubert et al., 2006; Reynolds et al., 2003; Riotte and Chabaux, 1999; Tricca et al., 2001), but are characterized by higher variability.

When a simple statistical treatment of the data is carried out, the main parameters controlling the uranium behavior and the distribution of the $(^{234}U/^{238}U)_{act}$ in the Becancour groundwater system are revealed (Fig. 4a–d). Groundwater located in the main recharge zone of the Appalachians is characterized by lower $(^{234}U/^{238}U)_{act}$ (median value of 2.64; n = 13 Fig. 4a) than those measured in the St. Lawrence Lowlands plain (median value of 3.79; n = 10 Fig. 4a), where groundwater discharges. Shallower granular aquifers show a $(^{234}U/^{238}U)_{act}$ median value of 1.26 (n = 3), closer to the secular equilibrium value (i.e., 1) than groundwater in the deeper fractured bedrock aquifer. Which shows higher $(^{234}U/^{238}U)_{act}$ (median value of 3.03; n = 20 Fig. 4b). There is an increase in the $(^{234}U/^{238}U)_{act}$ fractionation with hydrological conditions of the aquifer (Fig. 4c). Unconfined and semi-confined aquifers have lower $(^{234}U/^{238}U)_{act}$ (median value of 2.64, n = 16 and 2.50, n = 3; Fig. 4c) than confined aquifers (median value of 4.08, n = 4; Fig. 4c). Most importantly, the $(^{234}U/^{238}U)_{act}$ is found to progressively fractionate towards higher values in groundwater that is more chemically evolved (Fig. 4d). Ca–HCO_3 newly recharged water has the lowest $(^{234}U/^{238}U)_{act}$, with a median value of 2.31 (n = 12). The value is even lower (1.22) if only the 3 samples

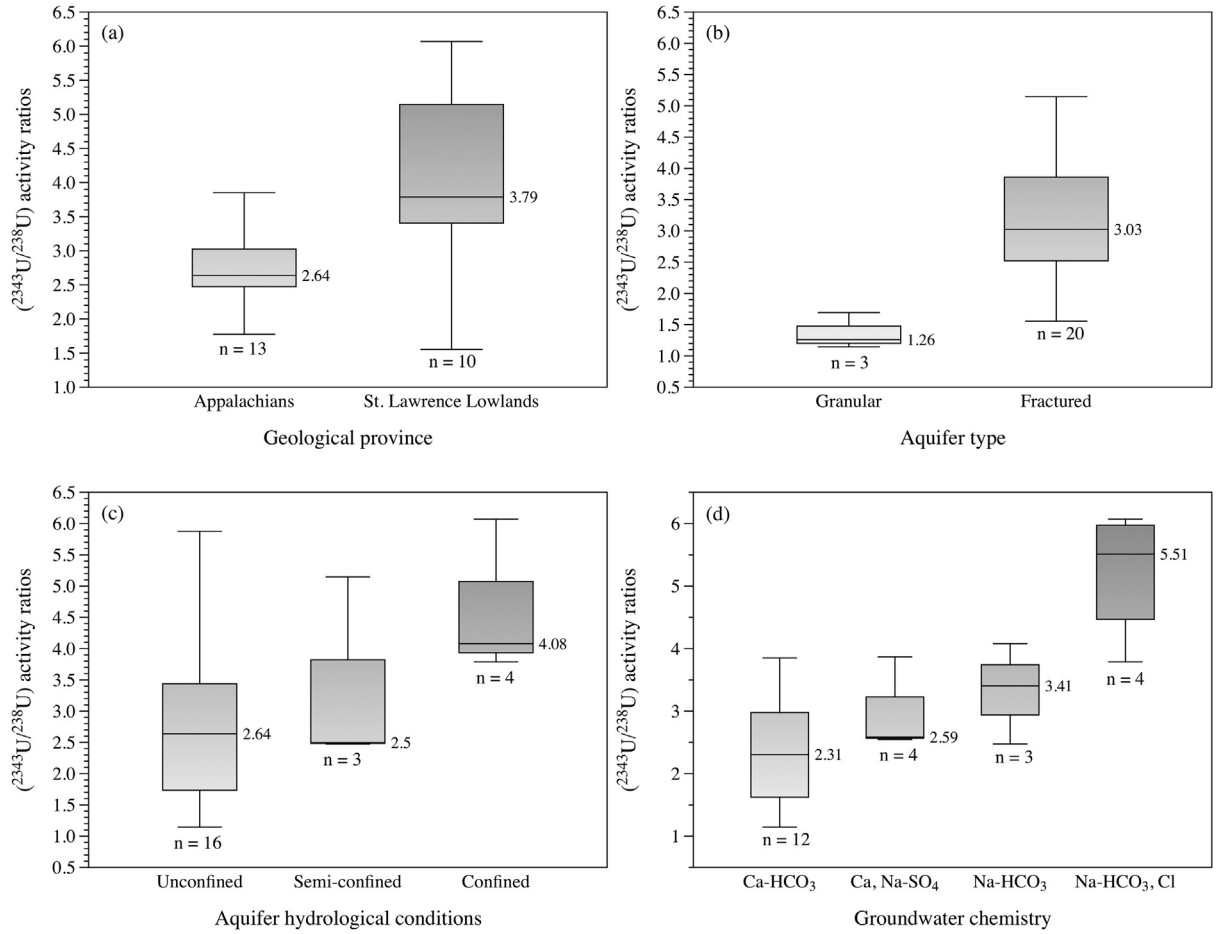

Fig. 4. Statistical boxplots of $(^{234}U/^{238}U)_{act}$ for Becancour watershed groundwater samples as a function of the geological province (a), aquifer type (b), hydrogeological conditions of aquifer (c), and groundwater chemistry (d).

from the shallowest granular aquifer with the youngest waters are considered. Older water, which exchanged Ca^{2+} with Na^{+}, has a fractionated $(^{234}U/^{238}U)_{act}$ median value of 3.41 (n = 3). Highly evolved Na–HCO_3–Cl water, representing post-glacial meltwater preserved in the fractured bedrock aquifer (Vautour et al., 2015), has a median $(^{234}U/^{238}U)_{act}$ value of 5.51 (n = 4). This water is slightly saline, with chlorine derived from trapped pore seawater (Meyzonnat et al., 2015).

5. Discussion

5.1. Uranium mobilization and redox conditions in the aquifers

The concentration of uranium in groundwater depends on aquifer redox conditions, which strongly impact the radionuclide transport in groundwater. The oxidized form, U^{+6}, reacts with O_2-rich freshwater and forms UO_2^{2+}, a highly mobile dissolved cation (Langmuir, 1978). ^{234}U and ^{238}U are brought into the water phase through the formation of uranyl complexes or U-fluoride complexes with carbonates and hydroxides under reduced conditions and above pH 7 to 8 (Chabaux et al., 2003). Under mildly reducing conditions, U^{+6} forms complexes with Cl and SO_4 in saline groundwater (Gascoyne, 1992). While progressing along its flow path and to confined conditions, groundwater becomes increasingly reduced by microbial aerobic respiration, which uses O_2 as an electron acceptor (Chapelle et al., 1995). The reduced form, U^{+4}, is rapidly adsorbed on the mineral surface of the aquifer matrix (Langmuir, 1978; Porcelli and Swarzenski, 2003), and thus is removed from groundwater.

In the absence of measured Eh or dissolved oxygen in the sampled groundwater, the concentration of SO_4 can be used as proxy of an aquifer's redox conditions, SO_4 being converted into

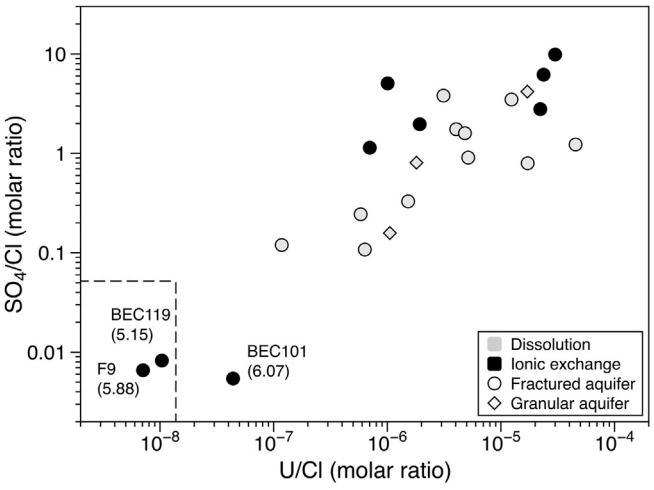

Fig. 5. U/Cl molar ratios as a function of SO_4/Cl ratios in Becancour watershed groundwater samples. The dotted lines represent the seawater U/Cl and SO_4/Cl ratios. Numbers in parentheses for BEC101, BEC119, and F9 are measured $(^{234}U/^{238}U)_{act}$.

insoluble sulfides under reducing conditions. Fig. 5 is a logarithmic plot of the measured SO_4/Cl versus U/Cl molar ratios, with Cl used to normalize values against dilution effects. There is a roughly linear trend, indicating that under increasingly reducing conditions, both SO_4 and U are removed from the groundwater system, the first by forming insoluble sulfides, which are then adsorbed on grain and mineral surfaces. It is interesting to note that the three water samples with the lowest SO_4 and U concentrations (Fig. 5) are BEC101, BEC119, and F9, which exhibit more fractionated $(^{234}U/^{238}U)_{act}$ (Table 1). The adsorbed U could constitute a local source of ^{234}U that is easily transferred in soluble form into the water phase, creating high ^{234}U–^{238}U fractionation (e.g., Ivanovich et al., 1991). However, the relationship between U- and He-isotopes seems to exclude this process as the one controlling the ^{234}U–^{238}U fractionation. Indeed, the possible amount of adsorbed U would be by far insufficient to explain the amount of radiogenic ^4He found in these samples (Table 1; see section 5.3 for details).

5.2. ^{234}U–^{238}U fractionation and the chemical evolution of the water

The following scenario might explain the observed trends in $(^{234}U/^{238}U)_{act}$ with regards to geological context, aquifer type, hydrological conditions, and water chemistry in the Becancour groundwater system (Fig. 4a–d). The main recharge zone in the Appalachian Mountains and the shallow granular aquifers (both in the Appalachian Mountains and in the plain) are dominated by recently recharged freshwater. This water dissolves carbonate minerals as it infiltrates, acquiring Ca–HCO_3 chemistry. Bulk dissolution of a mineral surface is a zero-order rate process that results in the incorporation of U having the same $(^{234}U/^{238}U)_{act}$ as the bulk solid (Bonotto and Andrews, 1993), which is close to secular equilibrium. Along the flow path, water evolves into Na–HCO_3 type when Ca^{2+}_{water} exchanges with $Na^{+}_{mineral}$ in semi-confined aquifers (Cloutier et al., 2006; Meyzonnat et al., 2015). Approaching the most confined portion of the fractured bedrock aquifer, water evolves to Na–HCO_3–Cl through exchange with saline pore water from the Champlain Sea clay (Cloutier et al., 2010). Na^+ is not a cation involved in the formation of complexes with uranium (uranyl ions), which might be responsible for transport of U into groundwater. However, there is a roughly linear trend between the measured $(^{234}U/^{238}U)_{act}$ and Na^+ in study area (Fig. 6a), which might suggest a causative relationship. The relationship between Na^+ and $(^{234}U/^{238}U)_{act}$ might, however, simply indicate mixing between the little-evolved Ca–HCO_3 waters, dominated by the dissolution of carbonates and U with an activity ratio close to secular equilibrium (U bulk dissolution), and more evolved, Na-rich waters, where U isotopic fractionation is produced by the preferential release of ^{234}U by α-recoil. This mixing is also apparent through the roughly linear relationship between the alkalinity of water (expressed here as mg L^{-1} of HCO_3 equivalent; Table 1) and the $(^{234}U/^{238}U)_{act}$ (Fig. 6b).

The relationships between $(^{234}U/^{238}U)_{act}$ and alkalinity, and $(^{234}U/^{238}U)_{act}$ and Na concentration (Fig. 6) could be interpreted either in terms of the time-dependent chemical evolution of the water and progressive accumulation of ^{234}U or in terms of the mixing of distinct sources. The second hypothesis appears to be more plausible. Indeed, if $(^{234}U/^{238}U)_{act}$ fractionation was a time-dependent process, an evolution along the flow path from the Appalachian recharge to the St. Lawrence River discharge would be expected, but this has been not observed. Well BEC118, which shows bulk dissolution and $(^{234}U/^{238}U)_{act}$ close to the secular equilibrium, is located downgradient in the St. Lawrence Plain, while elevated $(^{234}U/^{238}U)_{act}$ values have been observed both downgradient (BEC101) and upgradient (BEC126). This means that

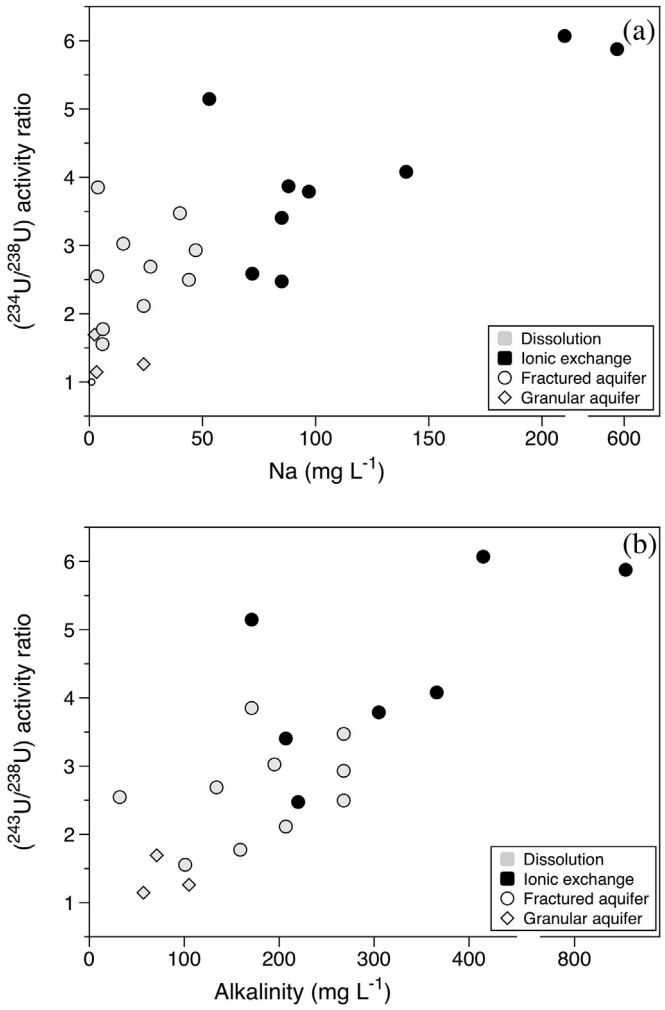

Fig. 6. Measured $(^{234}U/^{238}U)_{act}$ as a function of Na^+ concentration (a), and alkalinity (b). Diamonds represent groundwater from Quaternary granular aquifers. Circles represent groundwater from the Ordovician fractured bedrock, where samples whose chemistry is controlled by the dissolution of carbonates are shaded gray, and black symbols represents samples whose chemistry is controlled by ionic exchange processes.

$(^{234}U/^{238}U)_{act}$ evolved locally and discrete water masses with characteristic $(^{234}U/^{238}U)_{act}$ then mixed together.

If this mixing scenario could explain the distribution of ^{234}U–^{238}U fractionations in the watershed, the cause of this fractionation requires an explanation. $(^{234}U/^{238}U)_{act}$ ratios higher than 3 are generally observed in oxidizing groundwater with low circulation rates (small water/rock ratios) and with low etch rates (Bonotto and Andrews, 1993; Paces et al., 2002), or in deep reducing brines that have very low U concentrations where, in same rare cases, $(^{234}U/^{238}U)_{act}$ values up to 16 have been measured (Banner et al., 1990). In the Becancour watershed, groundwater has very low salinity, between 61 and 780 mg L^{-1} (Table 1), which excludes porewater of marine origin from being the main source of ^{234}U. Alternative processes producing ^{234}U–^{238}U fractionation in groundwater need to be explored.

5.3. He and U isotopes: groundwater mixing

Fig. 7 shows the $(^{234}U/^{238}U)_{act}$ plotted against the $^3He/^4He$ ratios (normalized to the atmospheric ratio, $Ra = 1.386 \times 10^{-6}$). This is one of the first times that these two sets of isotopes have been

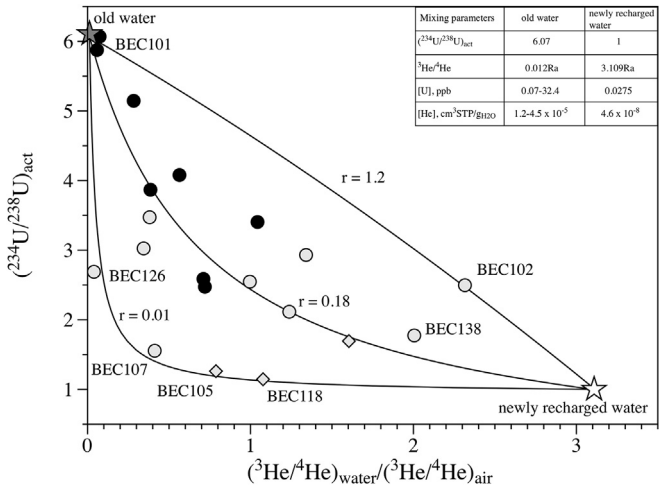

Fig. 7. Measured $(^{234}U/^{238}U)_{act}$ as a function of the $^{3}He/^{4}He$ ratios normalized to the same ratio measured in the air (Ra). Least-square mixing hyperbolas between an evolved water end-member, with $(^{234}U/^{238}U)_{act}$ of 6.07 and $^{3}He/^{4}He$ ratio of 0.012Ra, and a tritiogenic-rich freshwater end-member, with $(^{234}U/^{238}U)_{act}$ of ~1 and $^{3}He/^{4}He$ ratio of 3.109Ra, are also plotted. Values of hyperbola curvature, "r", are reported for each mixing curve. Symbols are as in Figs. 5 and 6.

investigated together in a groundwater system (e.g., Tokarev et al., 2006). The $^{3}He/^{4}He$ ratio would be atmospheric (1 Ra) or higher for groundwater recharging the system between the mid-1950s and the present-day, with ^{3}He excesses derived from the decay of post-bomb tritium (^{3}H) (Takaoka and Mizutani, 1987). Older water tends to have $^{3}He/^{4}He$ ratios of less than one because of the production of radiogenic ^{4}He from the decay of U and Th contained in the aquifer rock and its accumulation with time in the water (Torgersen and Clarke, 1985).

The ratio–ratio plot presented in Fig. 7 shows the mixing between at least two groundwater sources having distinct U and He isotopic signatures. The first end-member is an old water having accumulated large amount of radiogenic ^{4}He. The resulting $^{3}He/^{4}He$ ratio should be close to that expected for production from Li (^{3}He), U, and Th (^{4}He) present in local formations (0.012Ra; Pinti et al., 2011; Saby et al., 2016). The $(^{234}U/^{238}U)_{act}$ of the evolved water end-member is assumed to be equal to that of BEC101, which is the highest measured in the Becancour watershed. The second end-member is recently recharged water, containing ^{3}He in excess of its atmospheric concentration by production from tritium. The highest $^{3}He/^{4}He$ ratio measured in the Becancour groundwater is 3.10 ± 0.07 (Vautour et al., 2015), and is assumed in the current study to be the maximum reached in the watershed. The $(^{234}U/^{238}U)_{act}$ of the recently recharged water end-member should be close to one (i.e., U in the water is isotopically at secular equilibrium). Here, we assume for simplicity that $(^{234}U/^{238}U)_{act}$ is at secular equilibrium. Calculations on mixing hyperbola are not affected if a $(^{234}U/^{238}U)_{act}$ slightly higher than 1 is assumed.

For a general binary mixing model (Fig. 7), mixing lines are hyperbolas with the numerical value "r" = $([U]/[He])_A/([U]/[He])_B$ defining the degree of curvature between the two end-members, A and B (Langmuir et al., 1978). In Fig. 7, end-member A is the old water and end-member B is the recently recharged water. [U] and [He] are the uranium and helium concentrations (in molarity) measured in the two mixing end-members. Mixing curves will only be a straight line for the rare case where r = 1 (Langmuir et al., 1978).). It is worth noting that samples with Ca–HCO_3 type chemistry resulting from the dissolution of carbonate aquifer rocks (white circles; Fig. 7) are closer to the recently recharged water end-member, while mineralized Na–HCO_3 waters affected by ionic exchange are closer to the BEC101 end-member (black circles; Fig. 7).

With the exception of BEC102, BEC105, BEC107, BEC118, and BEC126, all other data define a common mixing trend, passing through the newly recharged and the older water end-members (Fig. 7). Using an inverse fitting method, as described in Albarede (1995; page 262), the resulting least-square mixing hyperbola has a curvature of 0.18. BEC126, BEC105, BEC107, and BEC118 lie on a different mixing hyperbola with a curvature of 0.01. BEC102 can be explained by a mixing hyperbola with a curvature of 1.2 (Fig. 7).

The two primary mixing trends revealed in Fig. 7 appear to be approximately similar to those observed by Vautour et al. (2015) in a plot of $^{3}He/^{4}He$ vs uncorrected ^{14}C ages. Water samples BEC126, BEC105, BEC107, and BEC118 defined a mixing trend alone between old and newly recharged waters. All the other samples defined a second mixing trend between BEC101 and BEC138 (Vautour et al., 2015). In terms of ^{234}U–^{238}U fractionation (Fig. 7), these trends might indicate the mixing of old water with newly recharged water infiltrated under different recharge conditions in terms of lithology (Chabaux et al., 2003) and/or infiltration rates (Tricca et al., 2001).

The obtained "r" values can add some insight as to the expected amounts of U in the older groundwater source, if the other concentrations are held fixed. Newly recharged waters are too young ($^{3}He/^{3}He$ ages of less than 50 yrs; Vautour et al., 2015) to have accumulated radiogenic ^{4}He produced from the aquifer rock. Here, we assume that the ^{4}He content in the freshwater is purely atmospheric in origin and is dissolved in water at the average temperature of the aquifer (ASW value at 10 °C of 4.59×10^{-8} $cm^3STP\ g^{-1}_{H2O}$). The [U] amount in the newly recharged water end-member should be lower than the amount measured in water samples (BEC138, BEC118) located on the right side of Fig. 7, i.e. < 0.0275 ppb. The [He] amount in the older water end-member is more difficult to estimate and could be highly variable. BEC101, which best represents the older water end-member (Fig. 7), has a ^{4}He concentration of 1.16×10^{-5} $cm^3STP\ g^{-1}_{H2O}$. BEC126 has highly variable concentrations, which might result from mixing with the theoretical older water end-member. Vautour et al. (2015) measured concentrations ranging from 2.6 to 4.5×10^{-5} $cm^3STP\ g^{-1}_{H2O}$ (Table 1). Here, we assume that the old water end-member could have [He] concentrations ranging from 1.2 to 4.5×10^{-5} $cm^3STP\ g^{-1}_{H2O}$. From the calculated curvature factors, "r", the U content in the old water end-member could range from between 0.07 and 0.3 ppb (r = 0.01) to between 1.3 and 4.9 ppb (r = 0.18). These values are within the range of or slightly higher than those measured in the Becancour watershed groundwater (Table 1). The amount of U needed to explain the relatively high $(^{234}U/^{238}U)_{act}$ measured in BEC102 would be excessively high, from 8.8 to 32.4 ppb. It is likely that this water sample is not a mixture of the two end-members defined above, but that it acquires this relatively high $(^{234}U/^{238}U)_{act}$ of 2.50 locally.

5.4. Processes leading to $(^{234}U/^{238}U)_{act}$ isotopic fractionation and radiogenic ^{4}He excesses

Vautour et al. (2015) observed that the amount of radiogenic ^{4}He measured in both BEC101 and BEC126 cannot be derived from the *in situ* decay of U and Th contained in the aquifer rocks. To obtain enough ^{4}He in groundwater from *in situ* production rates in fractured bedrock (3.5×10^{-13} $cm^3STP\ g^{-1}_{H2O}\ yr^{-1}$; Vautour et al., 2015), groundwater ages need to range from 379 ka for BEC101 to 1.45 Ma for BEC126, while ^{14}C adjusted ages are of 6.6 and 2.5 kyrs respectively (Vautour et al., 2015). Alternatively, assuming the ^{14}C-adjusted ages of BEC101 and BEC126 to be 6.6 and 2.5 kyrs, the bulk U and Th contents in the aquifer rocks should be on the order of 90–900 ppm [U] and 300–3000 ppm [Th] to produce the measured

radiogenic ^{4}He. These amounts are 10–100 times higher than average bulk U and Th amounts of 1.5 and 5.7 ppm measured in the aquifer rocks by Vautour et al. (2015).

The causal relationship between radiogenic ^{4}He and U isotopes in groundwater end-members requires a process able to simultaneously fractionate ^{234}U from ^{238}U as well as decrease the initial ^{3}He/^{4}He by adding large amounts of radiogenic ^{4}He. Stress-induced fracturing of the rock might be the cause of this process (Andrews et al., 1982; Andrews and Kay, 1983; Torgersen and O'Donell, 1991). An increase in rock fracturing could have taken place following ice retreat and the accelerated phase of isostatic rebound from 12 kyrs to 6.7 kyrs (Lamarche et al., 2007), increasing the permeability (e.g., Person et al., 2007; Aquilina et al., 2015), and shaping the hydrological network of the St. Lawrence Lowlands close to that observed at present (e.g., Lamarche et al., 2007; Saby et al., 2016).

Radiogenic helium is usually released by diffusion and α-recoil from the rock (Torgersen, 1980). If the aquifer rock grain size is much larger than the distance of α-recoil (30–100 μm; Torgersen, 1980) or than that of diffusion length, only a fraction of the produced ^{4}He will be released to the water phase, while the majority will accumulate into the rock for a long time (Solomon et al., 1996). Torgersen and O'Donnell (1991) have suggested that the progressive fracturing of a rock slab increases the specific surface exposed to water and therefore that the ^{4}He accumulated in the rock can be instantaneously released into the water. A 1-D model of rock fracturing showed that stress-induced macro-fracturing every 10 m along a 1 km wide rock slab would allow the release of ^{4}He otherwise accumulated over 15 Myrs in only 1500 years (Torgersen and O'Donnell, 1991).

Increasing the aquifer matrix surface area exposed to water by fracturing would also enhance the release of ^{234}U by α-recoil and thus shift the initial $(^{234}U/^{238}U)_{act}$ towards higher values. This process can be modeled following equation (1) of Andrews et al. (1982) (see also Andrews and Kay, 1983):

$$\left(\frac{^{234}U}{^{238}U}\right)_{act}^{final} = 1 + \left[\left(\frac{^{234}U}{^{238}U}\right)_{act}^{initial} - 1\right]\cdot e^{(-^{234}\lambda t)} + 0.235\cdot\rho\cdot S\cdot R\cdot\left[1 - e^{(-^{234}\lambda t)}\right]\cdot\frac{[U]_{rock}}{[U]_{water}} \quad (1)$$

In this equation, the first term is the decay of ^{234}U, while the second term is the production of ^{234}U in the rock (Andrews et al., 1982). $\left(\frac{^{234}U}{^{238}U}\right)_{act}^{final}$ is the final activity ratio measured for BEC101 (6.07) and $\left(\frac{^{234}U}{^{238}U}\right)_{act}^{initial}$ is the initial activity ratio assumed to be close or equal to the secular equilibrium value; $^{234}\lambda$ is the decay constant of ^{234}U (2.785×10^{-6} yr^{-1}); ρ is the rock density (2.72 g cm^{-3} for carbonates); R is the recoil length of ^{234}Th in the rock (3×10^{-6} cm) (Andrews and Kay, 1983); [U] is the uranium concentration in ppm in the rock (1.19 ppm for BEC101; Vautour et al., 2015) and in the water (0.0442 ppb for BEC101; Table 1); t is the groundwater residence time, reported here as the NETPATH adjusted ^{14}C age of 6696 yrs for BEC101 (Vautour et al., 2015); S is the fracture surface area (cm^2/cm^3), which is the rock surface in contact with a volume unit of groundwater (Andrews and Kay, 1983). It is proportional to the fracture width w ($w = 2/S$) and it is an indirect index of the extent of rock fracturing (Andrews and Kay, 1983; Elliot et al., 2014).

The extent of the ^{234}U–^{238}U isotopic fractionation measured in BEC101 ($(^{234}U/^{238}U)_{act} = 6.07 \pm 0.14$) can be explained by a density of fracturing S = 5296 cm^2 cm^{-3}, equivalent to a w of 3.8 μm. This fracture opening is consistent with the hydraulic conductivities measured during well pumping tests (Larocque et al., 2013). Fracture opening (w) is related to hydraulic conductivity (K_f) following the relationship (e.g., Witherspoon et al., 1980):

$$K_f = \frac{[(w^2)\times\varphi\times g]}{12\times\mu} \quad (2)$$

Where μ is the kinematic viscosity of water at aquifer temperatures (0.0013 kg/m/s); ρ is the density of water (assumed equal to 1); and g is the gravity acceleration. Calculated *Kf* is 2.4×10^{-8} m s^{-1} for BEC101, within the values measured in the Becancour fractured bedrock of $0.5–80 \times 10^{-8}$ m s^{-1} during well pumping tests (Larocque et al., 2013).

6. Conclusions

The goal of this study was to investigate the systematics of ^{234}U and ^{238}U isotopes in groundwater from the aquifers of the St. Lawrence Lowlands, to improve understanding of the chemical evolution of its waters. Results of this study showed that the measured variability in the ^{234}U/^{238}U activity ratios, which range from 1.14 ± 0.01 to 6.07 ± 0.14, is related to mixing of waters with distinct $(^{234}U/^{238}U)_{act}$, acquired locally.

The relationship between ^{3}He/^{4}He and $(^{234}U/^{238}U)_{act}$ reveal the occurrence of distinct water types with separate evolutionary origins: 1) modern freshwater located in the upper granular aquifer, poorly mineralized and with a $(^{234}U/^{238}U)_{act}$ close to the secular equilibrium, and 2) a mineralized older water from the fractured aquifer with a higher $(^{234}U/^{238}U)_{act}$ of 6.07.

The inverse causal relationship between helium isotope (^{3}He/^{4}He) and U isotope $(^{234}U/^{238}U)_{act}$ ratios (Fig. 7) suggests a unique common process, able to simultaneously fractionate $(^{234}U/^{238}U)_{act}$ toward higher values and lower the ^{3}He/^{4}He ratios, through a concomitant release of ^{234}U and ^{4}He. The underlying process might be rock fracturing, which is able to increase the surface area of rock exposed to α-recoil of ^{234}U and to α-recoil and diffusion of radiogenic ^{4}He, both mechanisms favoring the release of these two nuclides into the water phase. In future work, it would prove highly valuable to verify whether this He–U relationship exists in other hydrogeological contexts. Future work should also investigate the hypothesis that rock fracturing favors the release of large amounts of radiogenic helium from internal aquifer sources (Carey et al., 2004; Solomon et al., 1996), rather than being derived from the addition of helium basal fluxes from sources external to aquifers (Torgersen and Clarke, 1985).

Acknowledgments

We wish to thank the handling editor, Luc Aquilina, as well as J. Paces (USGS) and two anonymous reviewers for their thoughtful comments that greatly improved the manuscript. We also thank G.B. Johnson for correcting English, The authors thank the Quebec Ministry of Environment (*Ministère du Développement durable, de l'Environnement, des Parcs et de la Lutte contre les changements climatiques*), the Quebec Research Fund ("Fonds de recherche du Quebec - Nature et Technologies"), the Becancour River Watershed Organization ("organisme de bassin versant GROBEC"), and the municipalities that contributed to this research (Cré Centre-du-Québec, MRC d'Arthabaska, MRC de Bécancour, MRC de l'Erable, MRC de Nicolet-Yamaska, AGTCQ, Céged Thetford).

References

Albarede, F., 1995. Introduction to Geochemical Modeling. Cambridge University

Press, New York, USA.
Andersen, M.B., Erel, Y., Bourdon, B., 2009. Experimental evidence for ^{234}U–^{238}U fractionation during granite weathering with implications for $^{234}U/^{238}U$ in natural waters. Geochim. Cosmochim. Acta 73, 4124–4141.
Andrews, J.N., 1983. Dissolved radioelements and inert gases in geothermal investigations. Geothermics 12, 67–82.
Andrews, J.N., Giles, I.S., Kay, R.L.F., Lee, D.J., Osmond, J.K., Cowart, J.B., Fritz, P., Barker, J.F., Gale, J., 1982. Radioelements, radiogenic helium and age relationships for groundwaters from the granites at Stripa. Swed. Geochim. Cosmochim. Acta 46, 1533–1543.
Andrews, J.N., Kay, R.L.F., 1983. The U contents and $^{234}U/^{238}U$ activity ratios of dissolved uranium in groundwaters from some Triassic Sandstones in England. Chem. Geol. 41, 101–117.
Aquilina, L., Vergnaud-Ayraud, V., Armandine Les Landes, A., Pauwels, H., Davy, P., Pételet-Giraud, E.T., Roques, C., Chatton, E., Bour, O., Ben Maamar, S., Dufresne, A., Khaska, M., Le Gal La Salle, C., Barbecot, F., 2015. Impact of climate changes during the last 5 million years on groundwater in basement aquifers. Sci. Rep. 5, 14132.
Banner, J.L., Wasserburg, G.J., Chen, J.H., Moore, C.H., 1990. ^{234}U—^{238}U—^{230}Th—^{232}Th systematics in saline groundwaters from central Missouri. Earth Planet. Sci. Lett. 101, 296–312.
Benoit, N., Blanchette, D., Nastev, M., Cloutier, V., Marcotte, D., Brun Kone, M., Molson, J., 2011. Groundwater geochemistry of the lower Chaudière river watershed, Québec. In: GeoHydro2011, Joint IAH-CNC, CANQUA and AHQ Conference, Quebec City, Canada, August 28-31, 2011, Paper DOC-2209, p. 8.
Bonotto, D.M., Andrews, J.N., 1993. The mechanism of $^{234}U/^{238}U$ activity ratio enhancement in karstic limestone groundwater. Chem. Geol. 103, 193–206.
Bonotto, D.M., Andrews, J.N., 2000. The transfer of uranium isotopes ^{234}U and ^{238}U to the waters interacting with carbonates from Mendip Hills area (England). Appl. Rad. Isot. 52, 965–983.
Carey, A.E., Dowling, C.B., Poreda, R.J., 2004. Alabama Gulf Coast groundwaters: ^{4}He and ^{14}C as groundwater-dating tools. Geology 32, 289–292.
Castro, M.C., Ma, L., Hall, C.M., 2009. A primordial, solar He-Ne signature in crustal fluids of a stable continental region. Earth Planet. Sci. Lett. 279, 174–184.
Chabaux, F., Riotte, J., Dequincey, O., 2003. U-Th-Ra fractionation during weathering and river transport. Rev. Min. Geochem 52, 533–576.
Chapelle, F.H., McMahon, P.B., Dubrovsky, N.M., Fujii, R.F., Oaksford, E.T., Vroblesky, D.A., 1995. Deducing the distribution of terminal electron-accepting processes in hydrologically diverse groundwater systems. Water Resour. Res. 31, 359–371.
Chen, J.H., Edwards, R.L., Wasserburg, G.J., 1986. ^{238}U, ^{234}U, and ^{230}Th in seawater. Earth Planet. Sci. Lett. 80, 241–251.
Cherdyntsev, V.V., Chalov, P.I., Khasdarov, G.Z., 1955. On Isotopic Composition of Radioelements in Natural Objects, and Problems of Geochronology, 2012 Trans. 3rd Session of the Commission on Determination of Absolute Age of Geological Formations. Izv. Acad. Nauk SSR.
Cloutier, V., Lefebvre, R., Savard, M.M., Bourque, É., Therrien, R., 2006. Hydrogeochemistry and groundwater origin of the Basses-Laurentides sedimentary rock aquifer system, St. Lawrence Lowlands, Québec, Canada. Hydrogeol. J. 14, 573–590.
Cloutier, V., Lefebvre, R., Savard, M.M., Therrien, R., 2010. Desalination of a sedimentary rock aquifer system invaded by Pleistocene Champlain Sea water and processes controlling groundwater geochemistry. Environ. Earth Sci. 59, 977–994.
Durand, S., Chabaux, F., Rihs, S., Duringer, P., Elsass, P., 2005. U isotope ratios as tracers of groundwater inputs into surface waters: example of the Upper Rhine hydrosystem. Chem. Geol. 220, 1–19.
Edwards, R.L., Chen, J.H., Wasserburg, G.J., 1987. U-238, U-234, Th-230, Th-232 systematics and the precise measurement of time over the past 500,000 years. Earth Planet. Sci. Lett. 81, 175–192.
Elliot, T., Bonotto, D.M., Andrews, J.N., 2014. Dissolved uranium, radium and radon evolution in the Continental Intercalaire aquifer, Algeria and Tunisia. J. Environ. Radioact. 137, 150–162.
Fröhlich, K., 2013. Dating of old groundwater using uranium isotopes — Principles and applications. In: Isotope Methods for Dating Old Groundwater. International Atomic Energy Agency, Vienna, pp. 153–178.
Fröhlich, K., Gellermann, R., 1987. On the potential use of uranium isotopes for groundwater dating. Chem. Geol. 65, 67–77.
Gascoyne, M., 1992. Palaeoclimate determination from cave calcite deposits. Quart. Sci. Rev. 11, 609–632.
Gascoyne, M., 2004. Hydrogeochemistry, groundwater ages and sources of salts in a granitic batholith on the Canadian Shield, southeastern Manitoba. Appl. Geochem 19, 519–560.
Geyh, M., 2005. Dating of old groundwater—history, potential, limits and future. In: Aggarwal, P.K., Gat, J.R., Froehlich, K.F.O. (Eds.), Isotopes in the Water Cycle. Springer-Verlag, Berlin-Heidelberg, pp. 221–241.
Globensky, Y., 1993. Lexique stratigraphique canadien. Volume V-B: région des Appalaches, des Basses-Terres du Saint-Laurent et des Iles de la Madeleine. Ministère de l'Énergie et des Ressources et Direction Générale de l'Exploration géologique et minérale, p. 327. DV 91e23.
Godbout, P.-M., 2013. Géologie du quaternaire et hydrostratigraphie des dépôts meubles du bassin versant de la rivière Bécancour et des zones avoisinantes, Québec (MSc Thesis). Université du Québec à Montréal, Quebec, Canada.
Hillaire-Marcel, C., Causse, C., 1989. Chronologie Th/U des concrétions calcaires des varves du lac glaciaire de Deschaillons (Wisconsinien inférieur). Canad. J. Earth Sci. 26, 1041–1052.
Hubert, A., Bourdon, B., Pili, E., Meynadier, L., 2006. Transport of radionuclides in an unconfined chalk aquifer inferred from U-series disequilibria. Geochim. Cosmochim. Acta 70, 5437–5454.
Ivanovich, M., Fröhlich, K., Hendry, M.J., 1991. Uranium-series radionuclides in fluids and solids from the Milk River aquifer, Alberta, Canada. Appl. Geochem 6, 405–418.
Kigoshi, K., 1971. Alpha-recoil thorium-234: dissolution into water and the uranium-234/uranium-238 disequilibrium in nature. Science 173, 47–48.
Kronfeld, J., Gradsztajn, E., Müller, H.W., Radin, J., Yaniv, A., Zach, R., 1975. Excess ^{234}U: an aging effect in confined waters. Earth Planet. Sci. Lett. 27, 342–345.
Kronfeld, J., Gradsztajn, E., Yaniv, A., 1979. A flow pattern deduced from uranium disequilibrium studies for the Cenomanian carbonate aquifer of the Beersheva region, Israel. J. Hydrol. 44, 305–310.
Kulongoski, J.T., Hilton, D.R., 2011. Applications of groundwater helium. In: Baskaran, M. (Ed.), Handbook of Environmental Isotope Geochemistry. Springer-Verlag, Berlin-Heidelberg, pp. 285–303.
Lamarche, L., Bondue, V., Lemelin, J.-M., Lamothe, M., Roy, M., 2007. Deciphering the Holocene evolution of the St. Lawrence River drainage system using luminescence and radiocarbon dating. Quart. Geochronol. 2, 155–161.
Lamothe, M., 1989. A new framework for the Pleistocene stratigraphy of the central St. Lawrence Lowland, Southern Québec. Géogr. Phys. Quater. 43, 119–129.
Langmuir, D., 1978. Uranium solution-mineral equilibria at low temperatures with applications to sedimentary ore deposits. Geochim. Cosmochim. Acta 42, 547–569.
Langmuir, D., Vocke, R.D., Hanson, G.N., Hart, S., 1978. A general mixing equation with applications to Iceland basalts. Earth Planet. Sci. Lett. 37, 380–392.
Larocque, M., Gagné, S., Tremblay, L., Meyzonnat, G., 2013. Projet de connaissance des eaux souterraines du bassin versant de la rivière Bécancour et de la MRC de Bécancour. Quebec Ministry of Environment, p. 187. PACES Final Report. Available at: http://www.grobec.org/hydrogeo/pdf/Rapport_synthese_PACES_Bécancour_2013.pdf, (in French).
Lavoie, D., 2008. Appalachian Foreland Basin in Canada. In: Hsü, K.J., Miall, A.D. (Eds.), Sedimentary Basins of the World, Series Ed. Sedimentary Basins of the World — USA and Canada, 5. Elsevier, Amsterdam, pp. 65–103.
Maher, K., Steefel, C.I., DePaolo, D.J., Viani, B.E., 2006. The mineral dissolution rate conundrum: insights from reactive transport modeling of U isotopes and pore fluid chemistry in marine sediments. Geochim. Cosmochim. Acta 70, 337–363.
Meyzonnat, G., Larocque, M., Barbecot, F., Gagné, S., Pinti, D.L., 2015. The potential of major ion chemistry to assess groundwater vulnerability of a regional aquifer in southern Quebec (Canada). Environ. Earth Sci. http://dx.doi.org/10.1007/s12665-015-4793-9.
Occhietti, S., Richard, P.J.H., 2003. Effet réservoir sur les âges ^{14}C de la Mer de Champlain à la transition Pléistocène-Holocène : révision de la chronologie de la déglaciation au Québec méridional. Géogr. Phys. Quatern. 57, 115–138.
Occhietti, S., Chartier, H.M., Hillaire-Marcel, C., Cournoyer, M., Cumbaa, S.L., Harington, R., 2001. Paléoenvironnements de la Mer de Champlain dans la région de Québec, entre 11 300 et 9750 BP: le site de Saint-Nicolas. Géog. Phys. Quatern. 55, 23–46.
Osmond, J., Cowart, J., 1976. The theory and uses of natural uranium isotopic variations in hydrology. At. Energy Rev. 14, 621–679.
Osmond, J.K., Cowart, J., 1982. Natural uranium and thorium series disequilibrium: new approaches to geochemical problems. Nucl. Sci. Appl. B 1, 303–352.
Osmond, J.K., Cowart, J.B., 2000. U-series nuclides as tracers in groundwater hydrology. In: Cook, P., Herczeg, A. (Eds.), Environmental Tracers in Subsurface Hydrology. Kluwer Academic Publishers, Boston, pp. 145–174.
Osmond, J.K., Kaufman, M.I., Cowart, J.B., 1974. Mixing volume calculations, sources and aging trends of Floridan aquifer water by uranium isotopic methods. Geochim. Cosmochim. Acta 38, 1083–1100.
Ozima, M., Podosek, F.A., 1983. Noble Gas Geochemistry. Cambridge University Press, Cambridge, United Kingdom.
Paces, J.B., Ludwig, K.R., Peterman, Z.E., Neymark, L.A., 2002. $^{234}U/^{238}U$ evidence for local recharge and patterns of ground-water flow in the vicinity of Yucca Mountain, Nevada, USA. Appl. Geochem 17, 751–779.
Paces, J.B., Wurster, F.C., 2014. Natural uranium and strontium isotope tracers of water sources and surface water–groundwater interactions in arid wetlands – Pahranagat Valley, Nevada, USA. J. Hydrol. 517, 213–225.
Parent, M., Occhietti, S., 1988. Late Wisconsinan deglaciation and Champlain sea invasion in the St. Lawrence valley, Québec. Géogr. Phys. Quatern. 42, 215–246.
Person, M., McIntosh, J., Bense, V., Remenda, V.H., 2007. Pleistocene hydrology of North America: the role of ice sheets in reorganizing groundwater flow systems. Rev. Geophys. 45, 1–28.
Phillips, F., Castro, M., 2003. Groundwater dating and residence-time measurements. Treatise Geochem. 5, 451–497.
Pinti, D.L., Marty, B., 1998. The origin of helium in deep sedimentary aquifers and the problem of dating very old groundwaters. Geol. Soc. Spec. Publ. 144, 53–68.
Pinti, D.L., Béland-Otis, C., Tremblay, A., Castro, M.C., Hall, C.M., Marcil, J.-S., Lavoie, J.-Y., Lapointe, R., 2011. Fossil brines preserved in the St-Lawrence Lowlands, Québec, Canada as revealed by their chemistry and noble gas isotopes. Geochim. Cosmochim. Acta 75, 4228–4243.
Plater, A.J., Ivanovich, M., Dugdale, R.E., 1992. Uranium seriesdisequilibrium in river sediments and waters: the significance of anomalous activity ratios. Appl. Geochem 7, 101–110.
Plummer, L., Glynn, P., 2013. Radiocarbon dating in groundwater systems. In: Isotope Methods for Dating Old Groundwater. International Atomic Energy

Agency, Vienna, pp. 33–90.
Porcelli, D., Swarzenski, P.W., 2003. The behavior of U- and Th-series nuclides in groundwater. Rev. Mineral. Geochem 52, 317–361.
Reynolds, B.C., Wasserburg, G.J., Baskaran, M., 2003. The transport of U- and Th-series nuclides in sandy confined aquifers. Geochim. Cosmochim. Acta 67, 1955–1972.
Riotte, J., Chabaux, F., 1999. ($^{234}U/^{238}U$) activity ratios in freshwaters as tracers of hydrological processes: the Strengbach watershed (Vosges, France). Geochim. Cosmochim. Acta 63, 1263–1275.
Riotte, J., Chabaux, F., Benedetti, M., Dia, A., Gérard, M., Boulègue, J., Etamé, J., 2003. Uranium colloidal transport and origin of the $^{234}U–^{238}U$ fractionation in surface waters: new insights from Mount Cameroon. Chem. Geol. 202, 365–381.
Saby, M., Larocque, M., Pinti, D.L., Barbecot, F., Sano, Y., Castro, M.C., 2016. Linking groundwater quality to residence times and regional geology in the St. Lawrence Lowlands, southern Quebec. Can. Appl. Geochem 65, 1–13.
Solomon, D., Hunt, A., Poreda, R., 1996. Source of radiogenic helium 4 in shallow aquifers: implications for dating young groundwater. Water Resour. Res. 32, 1805–1813.
Takaoka, N., Mizutani, Y., 1987. Tritiogenic ^{3}He in groundwater in Takaoka. Earth Planet. Sci. Lett. 85, 74–78.
Torgersen, T., 1980. Controls on pore-fluid concentration of ^{4}He and ^{222}Rn and the calculation of $^{4}He/^{222}Rn$ ages. J. Geochem. Explor. 13, 57–75.
Torgersen, T., Clarke, W.B., 1985. Helium accumulation in groundwater, I: an evaluation of sources and the continental flux of crustal ^{4}He in the Great Artesian Basin, Australia. Geochim. Cosmochim. Acta 49, 1211–1218.
Torgersen, T., O'Donnell, J., 1991. The degassing flux from the solid earth: release by fracturing. Geophys. Res. Lett. 18, 951–954.
Torgersen, T., Stute, M., 2013. Helium (and other noble gases) as a tool for understanding long timescale groundwater transport. In: Isotope Methods for Dating Old Groundwater. International Atomic Energy Agency, Vienna, pp. 179–216.
Tokarev, I., Zubkov, A.A., Rumynin, V., Polyakov, V.A., Kuznetsov, V.Y., Maksimov, F.E., 2006. Origin of high $^{234}U/^{238}U$ ratio in post-permafrost aquifers. In: Merkel, B.J., Hasche-Berger, A. (Eds.), Uranium in the Environment. Springer-Verlag, Berlin Heidelberg, pp. 847–856.
Tran Ngoc, T.D., Lefebvre, R., Konstantinovskaya, E., Malo, M., 2014. Characterization of deep saline aquifers in the Bécancour area, St. Lawrence Lowlands, Quebec, Canada: implications for CO_2 geological storage. Environ. Earth Sci. http://dx.doi.org/10.1007/s12665-013-2941-7.
Tricca, A., Porcelli, D., Wasserburg, G.J., 2000. Factors controlling the groundwater transport of U, Th, Ra and Rn. Proc. Ind. Acad. Sci. Earth Planet. Sci. 109, 95–108.
Tricca, A., Wasserburg, G.J., Porcelli, D., Baskaran, M., 2001. The transport of U- and Th-series nuclides in a sandy unconfined aquifer. Geochim. Cosmochim. Acta 65, 1187–1210.
Vautour, G., Pinti, D.L., Saby, M., Méjean, P., Meyzonnat, G., Larocque, M., Castro, M.C., Hall, C.M., Barbecot, F., Boucher, C., Roulleau, E., Takahata, N., Sano, Y., 2015. $^{3}H/^{3}He$, ^{14}C and (U-Th)/He groundwater ages in the St. Lawrence Lowlands, Quebec. East. Can. Chem. Geol. 413, 94–106.
Witherspoon, P.A., Wang, J.S.Y., Iwai, K., Gale, J.E., 1980. Validity of cubic law for fluid flow in a deformable rock fracture. Water Resour. Res. 16, 1016–1024.